

# Sources and transport of the Deep Western Boundary Current east of the Kerguelen Plateau

Kathleen A. Donohue

University of Hawaii, Honolulu

Gwyneth E. Hufford, Michael S. McCartney

Woods Hole Oceanographic Institution, Woods Hole, Massachusetts

**Abstract.** East of the Kerguelen Plateau, a deep western boundary current in the Australian-Antarctic Basin brings cold dense waters north from the margins of Antarctica. Geostrophic velocities referenced to acoustic Doppler current profiler data, both shipboard and lowered, suggest the flow is unidirectional throughout the water column with estimated northwestward transport below potential temperature  $1^{\circ}\text{C}$  of  $28 \pm 7 \times 10^6 \text{ m}^3 \text{ s}^{-1}$  and  $49 \pm 9 \times 10^6 \text{ m}^3 \text{ s}^{-1}$ , respectively. Hydrographic and acoustic Doppler current profiler data show that the deep boundary current is supplied by northward flow emerging from the confluence of westward flow along the Antarctic continental slope and eastward flow of Weddell Basin waters through the Princess Elizabeth Trough to the south of the Kerguelen Plateau.

## 1. Introduction

The Antarctic Circumpolar Current (ACC) is believed to inhibit exchange between the southern high-latitude cold water sources and the mid-latitude adjacent oceans. Partial western boundaries in the Southern Ocean, such as the Antarctic Peninsula in the South Atlantic sector and the Kerguelen Plateau in the Indian Ocean sector, provide potential sites for western boundary currents and adjacent circulation gyres that could bring waters from the southern high-latitudes to join with the ACC. World Ocean Circulation Hydrographic Program sections I8S, I9S, completed aboard the R/V Knorr during December 1994 and January 1995, provide two quasi-meridional crossings of the Southern Ocean between the southern coast of Australia and the Adelie Coast of Antarctica (Figure 1). This paper provides a preliminary analysis of the transport and water-mass origins of the Deep Western Boundary Current (DWBC) in the Australia-Antarctic Basin (AAB) which flows northwestward along the eastern flank of the Kerguelen Plateau.

## 2. Data and Transport Calculation

In addition to full water column conductivity and temperature profiles and a suite of nutrient measurements, two independent direct-velocity measurements were taken using acoustic Doppler current profilers (ADCPs). A shipboard shipboard acoustic Doppler profiler (SADCP) continuously measured the upper-ocean currents. In addition, a lowered ADCP (LADCP) mounted on the underwater hydrographic

frame provided full ocean depth profiles of horizontal currents at each station. Details regarding the LADCP instrument and LADCP data processing may be found in *Hacker et al.* [1996] and *Fischer and Visbeck* [1993].

We calculate geostrophic velocities by referencing to a level of no motion (LNM) and to SADCP and LADCP data. The SADCP reference is determined by matching the relative geostrophic velocity to the average SADCP cross-track velocity in the depth range 200-400 m. The LADCP reference is determined by matching the geostrophic velocity to the mean, depth-averaged cross-track LADCP velocity for each station pair over the middle half of the water column. Instrument error in each depth-averaged LADCP profile are near  $1.0 \text{ cm s}^{-1}$  [*Hacker et al.*, 1996]. Calibration of the SADCP angular offset error from watertrack calibrations yields an overall error ( $2\sigma$ ) of  $0.06^{\circ}$  which results in an cross-track velocity uncertainty of  $0.6 \text{ cm s}^{-1}$  for a ship speed of 10 knots. The barotropic tide determined from the TPX0.3 global tidal model [*Egbert et al.*, 1994] is removed from the ADCP measurements and for the regions considered in this note are less than  $2 \text{ cm s}^{-1}$ . An ageostrophic between-station error of  $1.5 \text{ cm s}^{-1}$  is assumed for the both ADCP-references. We assume that the instrument error is correlated station-to-station while the ageostrophic error is uncorrelated station-to-station. Bottom triangles are filled by extending the deepest common level velocity.

## 3. DWBC Transport

*Speer and Forbes* [1994], identified the DWBC along the eastern flank of the Kerguelen Plateau from its geostrophic shear signature and water-mass properties. Along their sec-

**Table 1.** Geostrophic transports in Sv as a function of theta (rows) and geostrophic reference technique (columns) for the DWBC (stations 63 through 72) below  $1.0^{\circ}\text{C}$ .

	1500 dbar	2500 dbar	bot.	SADCP	LADCP
1.0 to 0.5	-0.2	1.1	3.1	-4.6 $\pm$ 1.7	-8.4 $\pm$ 2.5
0.5 to 0.0	-2.0	0.3	3.2	-8.4 $\pm$ 1.9	-14.5 $\pm$ 2.3
0.0 to -0.5	-8.1	-3.6	1.4	-15.0 $\pm$ 3.2	-26.0 $\pm$ 4.4
1.0 to -0.5	-10.3	-2.2	7.7	-28.0 $\pm$ 6.7	-48.9 $\pm$ 9.4

Positive values are southeastward. Upper-ocean transports (depths less than 500 m) are not included. Total transport for the three theta classes are given in the bottom row.

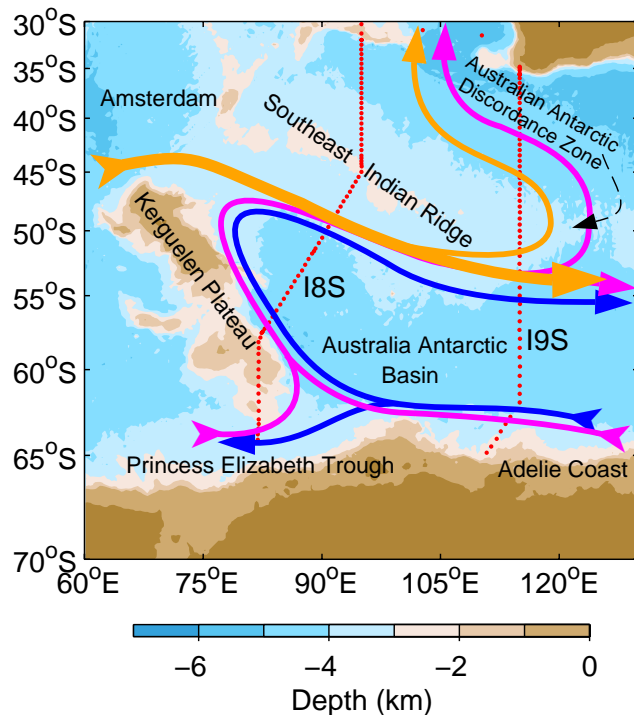


**Figure 1.** Circulation scheme for deep flow. Deep water ( $\theta > 1.0^\circ\text{C}$ , orange) in the ACC passes north of Kerguelen Plateau and traverses the AAB. The southern sources of colder ( $0.1 < \theta < 0.0^\circ\text{C}$ , pink) and coldest ( $\theta < 0.1^\circ\text{C}$ , blue) include a convergent flow into the DWBC off Kerguelen Plateau, and a subsequent eastward turn beneath the ACC. Part of the combined flow passes through a gap in the Southeast Indian Ridge and thence flows northward into the mid-latitude Indian Ocean [Hufford et al., 1997]. Station positions of the WHP sections I8S and I9S are in red.

tion, isopycnals rise steeply towards the Plateau indicating strong vertical shear. The near-bottom coldest waters must derive from a southern source and flow northward, and given the sense of geostrophic shear this requires a LNM above these waters. Speer and Forbes [1994] determine transport estimates for the DWBC for several choices of a LNM and conclude that the transport based upon a 2500 m LNM of 6 Sv ( $1 \text{ Sv} \equiv 10^6 \text{ m}^3 \text{ s}^{-1}$ ) is the best estimate. Shallower LNM choices yielded larger transports beneath the LNM but their assumption that upper-ocean waters above the DWBC flow southeast led to placing an upper limit of 10 Sv on the DWBC transport. Observations presented in the following indicate that the latter constraint is incorrect.

I8S extended from Broken Ridge across the Southeast Indian Ridge to the Kerguelen Plateau, and then southward into the PET as far as the ice edge. Isotherms in the AAB show a general southward rise with a sharp rise of isotherms towards the Plateau for station 65 through station 68 (Figure 2), similar to Speer and Forbes [1994]. (In this region, temperature gradients can be viewed as a proxy for density gradients.) In the northern AAB, the southward rise of isotherms is associated with the deep-reaching ACC fronts and a LNM is commonly placed at or near the bottom to send these waters southeastward. Deep waters brought into the AAB by the ACC in the passage between the northern Kerguelen Plateau and Amsterdam Island are as cold as  $\theta 0.87^\circ\text{C}$  [Park et al., 1993]. Therefore, deep water colder than  $0.87^\circ\text{C}$  along I8S must come from a region

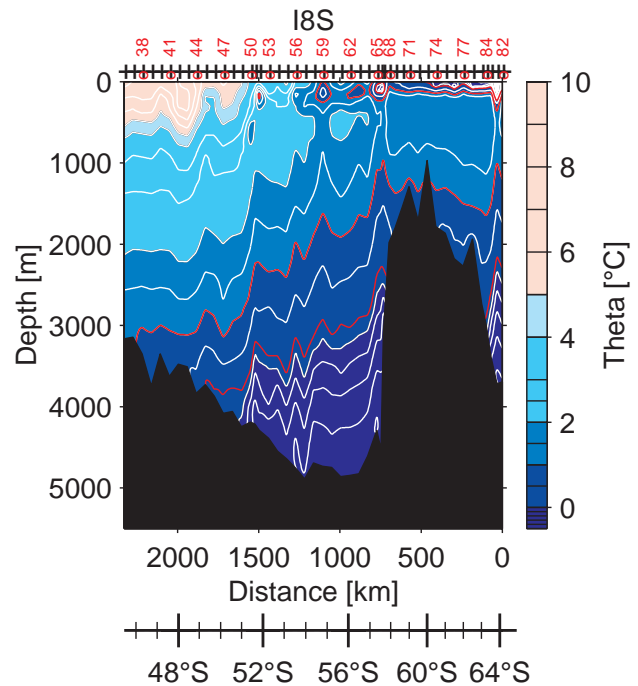


**Figure 2.** Theta along WHP section I8S from the Southeastern Indian Ridge across the Australian-Antarctic Basin, the Kerguelen Plateau and the Princess Elizabeth Trough. Contours for theta of  $1.0^\circ\text{C}$  and  $0.1^\circ\text{C}$  are colored red.

southeast of the section, and this requires a LNM above the cold water in the DWBC regime.

We define the horizontal boundaries of the DWBC as stations 63 to 72. The determination of the boundary in the eddy-rich background flow field is ambiguous, but the LADCP profiles (not shown) indicate general southeastward

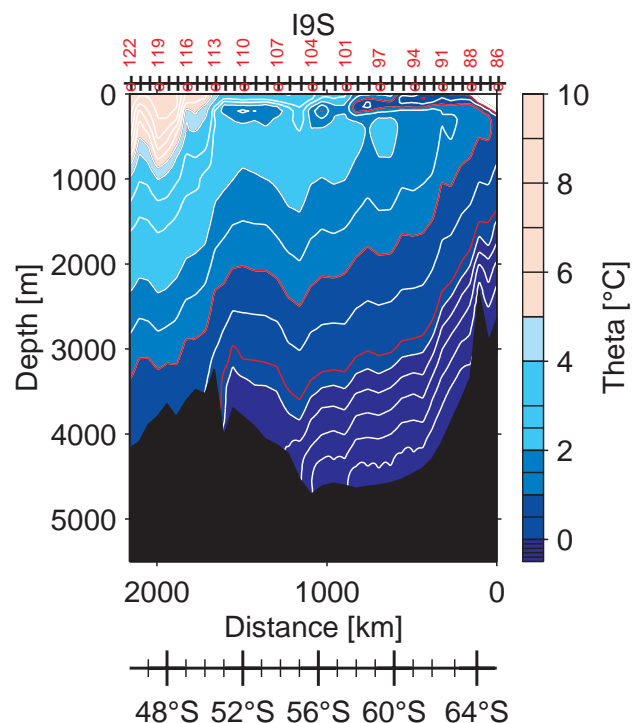


**Figure 3.** Theta along WHP section I9S from the Southeastern Indian Ridge, the Australian-Antarctic Basin to the continental slope of Antarctica. Contours for theta of  $1.0^\circ\text{C}$  and  $0.1^\circ\text{C}$  are colored red.

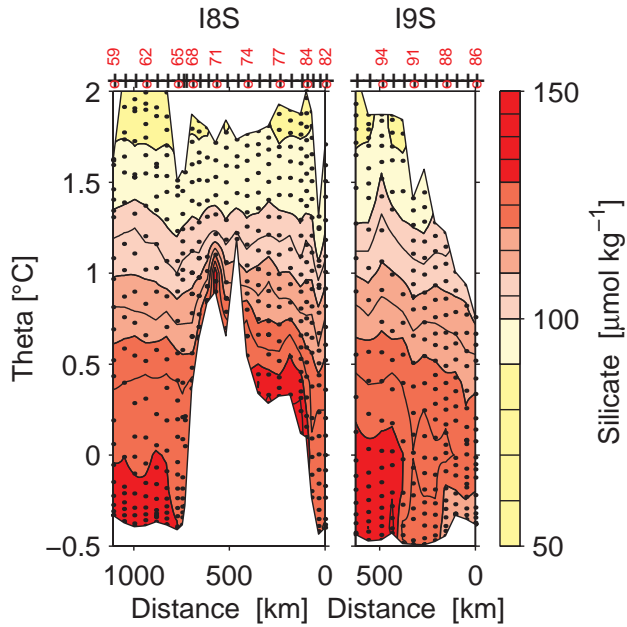


**Figure 4.** Silicate contoured against theta for the I8S section stations 59 to 84 (right panel) and I9S sections stations 85 to 96 (left panel). Depths less than 500 m are not included.

flow north of station 64 and northwestward flow from station 64 to station 72. (A few single-station reversals from the southeastward flow are associated with the visible isotherm reversals.) To focus on water of unambiguous southern origin, we report transports for water colder than theta 1°C (excluding near-surface waters). Our DWBC transport estimates are generally northwestward except when a deep LNM is used (Table 1). In contrast with *Speer and Forbes* [1994], the direct-velocity measurements indicate that the surface

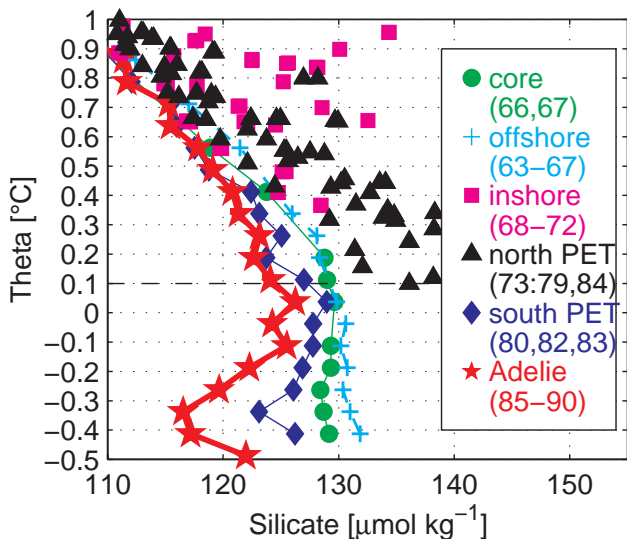


**Figure 5.** Silicate-theta plot. DWBC core (dots), offshore DWBC (crosses), southern PET (diamonds), and Adelle (stars) stations have been averaged. Inshore DWBC (squares) and northern PET (triangles) are not averaged. Depths less than 500 m are not included.

**Table 2.** Same as Table 1 but for the northern PET (stations 73 through 79,84,80) below 1.0°C.

	1500 dbar	2500 dbar	bot.	SADCP	LADCP
1.0 to 0.5	0.1	0.0	0.3	2.0±1.9	3.6±3.8
0.5 to 0.0	-0.3	-0.1	0.3	1.3±0.9	2.5±1.2
0.0 to -0.5	-0.3	-0.1	0.0	0.2±0.2	0.4±0.2
1.0 to -0.5	-0.5	-0.2	0.6	3.5±2.8	6.5±4.2

Positive values are eastward.

flow in the region of the DWBC is in the same direction as the DWBC and examination of individual LADCP profiles (not shown) in the DWBC core (stations 65-67) confirm that the flow is in the same direction at all depths; geostrophic transports based upon a LNM will consequently underestimate the transport in the DWBC. The northwestward DWBC transport estimates are 28±7 Sv and 49±9 Sv for the SADCP and LADCP referenced velocity, respectively while the 2500 dbar LNM northwestward transport is only 2 Sv.

#### 4. PET Transport

The Weddell gyre is one possible source for the DWBC. Cold water could flow east through the PET. Initial analysis of the I8S section suggested eastward flow in the northern PET [*Hufford and McCartney*, 1997] and *Heywood et al.* [1997] report eastward transport in the northern PET with strong bottom velocities associated with deep reaching ACC fronts and westward transport in the southern PET.

Crossing the Plateau, isotherms along I8S descend to the south well into the PET to station 84 before rising steeply to station 83 then descend again to the ice edge (Figure 2). (The station sequence from north to south is 73 to 79,84,80,83,82.) Assuming a deep or bottom LNM in the PET, our section suggests strong eastward flow for northern PET stations 84,80,83 associated with southward rising isotherms (which would bring Weddell Gyre waters to the AAB) and westward flow in the southern PET (stations 83,82). In northern PET, stations 73 to 79,84,80, the ADCP-referenced transport is to the east, 4±3 Sv for the SADCP, and 7±4 Sv for the LADCP (Table 2). About half the eastward transport occurs between station pair 84-80 for both ADCP references. A bottom LNM results in weak eastward transport. Our section does not fully extend across the PET, so we have not fully sampled the westward flow

**Table 3.** Same as Table 1 but for the Adelle Coast (stations 85 through 91) below 1.0°C.

	1500 dbar	2500 dbar	bot.	SADCP	LADCP
1.0 to 0.5	0.5	1.8	2.9	-3.4±1.9	-2.5±2.6
0.5 to 0.0	-0.4	1.8	3.1	-4.8±2.6	-4.5±4.8
0.0 to -0.5	-4.7	-0.9	1.6	-12.8±4.3	-11.3±5.8
1.0 to -0.5	-4.6	2.7	7.6	-21.0±8.1	-17.3±11.6

Positive values are eastward.

regime in the southern PET. Westward transports from stations 80,83,82 referenced to the SADCP and LADCP are  $5\pm 3$  Sv and  $3\pm 3$  Sv, respectively.

## 5. Adelie Coast Transport

The second possible source for the DWBC waters is westward flow along the continental slope of Antarctica. The I9S section, Figure 3, shows a general southward rise of isotherms and thus a single sign of geostrophic shear. The LADCP data (not shown) indicate deep westward flow for stations 85-91 and general eastward flow north of station 91 (with again, some flow reversals where the isotherms reverse slope.) The reversal of flow in a region where the sign of the shear is in the same direction suggests a south-to-north shift from a shallow LNM (westward deep flow near the Adelie Coast) to a bottom LNM (eastward deep flow in the ACC). There is a deep water-mass transition at station 91, discussed below, which also supports the idea of flow reversal. Table 3 shows geostrophic transport estimates for the westward flow regime along the Adelie Coast from I9S. Westward transport in the deep cold water is  $21\pm 8$  Sv and  $17\pm 12$  Sv for the SADCP and LADCP references, respectively. In contrast, a LNM of 1500 dbar gives far weaker westward transport of 5 Sv.

## 6. Origins of the DWBC

Deep nutrient properties show a vertical layering of water masses and onshore-offshore transitions across the DWBC east of Kerguelen Plateau.

In the DWBC core stations, 66-67, the deep waters are consistently lower in silicate at a given theta than further north (Figure 4 and Figure 5). We attribute this minima to waters deriving from the westward flow along the Antarctic continental slope where low silicate concentration are seen in the theta range  $-0.3^{\circ}\text{C}$  to  $-0.4^{\circ}\text{C}$  (Figures 4 and 5). Low silicate in this theta range is a general feature of deep waters near Antarctica, stemming from the plumes of dense, nutrient-depleted deep water formed near the shelves. The water-mass transition on I9S from low silicate water in the south to higher concentrations occurs near station 91 where the LNM shifts. The westward flow regime in the southern PET also shows low silicate for the same theta range although not as extreme as the Adelie stations (Figure 5). Interior waters from the Weddell Sea are not plausible sources for the deep cold DWBC waters because water in this theta range  $-0.3^{\circ}$  to  $-0.4^{\circ}\text{C}$  are not found in the eastward flow regime in the northern PET (the coldest waters flowing east there are theta  $0.1^{\circ}\text{C}$ ). Furthermore the interior waters for the Weddell Sea have silicate values that are too high, (e.g. Mantyla and Reid [1995], Figure 2e).

Inshore of the DWBC core, silicate levels systematically rise; high values are found over the southern Kerguelen Plateau (Figure 4). The ADCP-referenced DWBC transports (Section 3) yielded significant northward transport in theta class  $1.0^{\circ}$  to  $0.0^{\circ}\text{C}$ . Waters warmer than theta  $0.1^{\circ}\text{C}$  inshore of the DWBC core, stations 68-72, are similar to those found in the northern PET where the ADCP-referenced velocities show eastward flow (coldest theta  $0.1^{\circ}\text{C}$ ) and dissimilar to those found along the Adelie Coast (Figure 5).

## 7. Conclusions

Westward deep flow along the Antarctic continental slope, with ultimate origins in deep water formed in the Ross Sea and along the Adelie Coast, bifurcates in the southwestern AAB to supply both a westward branch through the southern PET into the Weddell-Enderby Basin and a northward branch into the DWBC off the Kerguelen Plateau (Figure 1). The latter branch is the sole source for northward DWBC flow with theta less than  $0.1^{\circ}\text{C}$ , but for theta greater than  $0.1^{\circ}\text{C}$  this northward branch converges with an eastward flow of Weddell waters passing through the northern PET as a combined source for DWBC flow.

The large DWBC transport exceeds the combination of PET and Adelie input transports and this implies a deep cyclonic recirculation system in the AAB. The inferred gyre may extend to the surface since ADCP measurements indicate that the DWBC is part of an unidirectional western boundary current. This western boundary current turns eastward, augmenting the ACC with DWBC waters ending up beneath the ACC (Figures 2,3).

**Acknowledgments.** Thanks to all the participants of the first WHP leg of R/V Knorr's WOCE expedition to the Indian Ocean, but particularly to Tom Whitworth, Eric Firing, Joe Jennings, and Marshall Swartz for their valuable contributions to a successful cruise. The hydrographic work was supported by NSF grant OCE-9413167 and ADCP work by NSF grant OCE-9413172. The analysis work by GEH and MSM was supported by NSF grant OCE-9711875. This is WHOI contribution 9834, SOEST contribution 4730, and WOCE contribution 577.

## References

- Egbert, G. D., A. F. Bennett, and M. G. G. Foreman, TOPEX/POSEIDON tides estimated using a global inverse model, *J. Geophys. Res.*, *99*, 24821-24852, 1994.
- Fischer, J. and M. Visbeck, Deep velocity profiling with self-contained ADCPs, *J. Ocean. Tech.*, *10*, 764-773, 1993.
- Hacker, P., E. Firing, W.D. Wilson and R. Molinari, Direct observations of the current structure east of the Bahamas, *Geophys. Res. Lett.*, *23*, 1127-1130, 1996.
- Heywood, K.J., M.D. Sparrow, J. Brown and R.R. Dickson, Frontal structure and Antarctic Bottom Water Flow through the Princess Elizabeth Trough, Antarctica, *in press*, *46*, *Deep-Sea Res.*, 1999.
- Hufford, G.E., and M.S. McCartney, Deep circulation southwest of Australia, *International WOCE Newsletter*, *25*, 31-35, 1997.
- Hufford, G.E., M.S. McCartney and K.A. Donohue, Northern boundary currents and adjacent recirculations off southwestern Australia, *Geophys. Res. Lett.*, *24*, 2797-2800, 1997.
- Mantyla, A.W., and J.L. Reid, On the origins of deep and bottom waters of the Indian Ocean, *J. Geophys. Res.*, *100*, 2417-2439, 1995.
- Park, Y.H., L. Gamberoni, and E. Charriaud, Frontal structure, water masses and circulation in the Crozet Basin, *J. Geophys. Res.*, *98*, 12,361-12,385, 1993.
- Speer, K.G., and A. Forbes, A deep western boundary current in the South Indian Basin, *Deep-Sea Res.*, *41*, 1289-1303, 1994.

K. Donohue, 1000 Pope Road, Honolulu, HI 98622. (e-mail: kathyd@soest.hawaii.edu)

G. Hufford and M. McCartney, Woods Hole Oceanographic Institution, Woods Hole, MA, 02543. (e-mail: gpackard@whoi.edu; mmcarter@whoi.edu)

(Received September 9, 1998; accepted October 20, 1998.)